

Extracting the Star Formation History of Composite Stellar Populations

Jenny Richardson

29/03/07

1 What is a Composite Stellar Population?

A simple stellar population (SSP) consists of stars with uniform age and metallicity formed by a single short-lived burst of star formation within a cloud of given chemical composition. Globular clusters and elliptical galaxies are good examples. By contrast, a composite stellar population (CSP) is one which contains stars formed at different times with varying initial chemical compositions. Disk galaxies, for instance, contain multiple generations of stars with manifold initial metal enrichments. A CSP is characterized by its star formation history (SFH) which depends on the star formation rate (SFR) and chemical enrichment law (CEL) as functions of time.

2 Why Extract the Star Formation History of a CSP?

In general, galaxy evolution proceeds dynamically through interactions, accretions and mergers with other dark matter halos and through the formation and evolution of the stars within them. Galaxy mergers, and interactions with dwarf satellite galaxies, may impact on the local star formation rate or add material as the disrupted satellite trails tidal debris along its orbit. All this information is contained within the CSP of a given field like a fossil record. Retrieving the SFH from the colour magnitude diagram (CMD) of such a population provides the empirical basis upon which robust theories of galaxy formation can be built. Here SFH refers to the star formation rate as a function of time, $SFR(t)$, and the chemical enrichment law as a function of time, $CEL(t)$. For example, extracting the SFH of composite stellar populations in galactic halo substructure can test the paradigm of hierarchical galaxy formation which predicts a large fraction of stellar halos should be built up by material from accreted sub halos. Alternatively, the SFH of isolated dwarf galaxies could be useful to explore the influence of re-ionisation on galaxy formation at high redshift.

3 The Expected Distribution of Disk Galaxy Stellar Populations

In a rough sense, different kinds of stars are distributed within the parent galaxy according to its components (thin disk, thick disk, bulge, halo etc.). Figure 1 shows the characteristic ages and metallicities expected of different components. (Here metallicity refers to $[Fe/H]$ by assuming a constant solar heavy metal distribution). Observations

show a gradient in age, metallicity and abundance of stars in thin disks extending to very young stars ($\leq 1\text{Gyr}$) with high metallicities. Bulges consists of old ($\geq 10\text{Gyr}$) relatively metal rich stars. Metal-weak thick disks can be as metal poor as Galactic globular clusters and are typically $\sim 10\text{Gyr}$ old. The evolution of these populations depends on

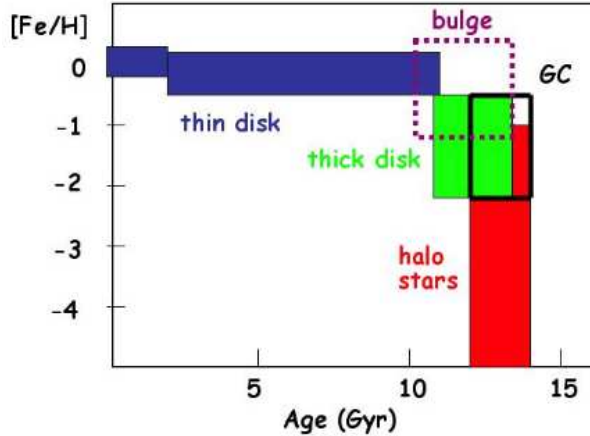


Figure 1: A simplified summary of the age-metallicity distribution of various components of the Galaxy. Taken from fig 2, Freeman and Bland-Hawthorn (2002).

the local environment (e.g., winds, infall of fresh material) which dictates the chemical enrichment law and star formation rate. They are far removed from the idealised case of a SSP. Naively one would expect to find exclusively ancient, metal poor populations in stellar halos, but the picture gets even more chaotic. The galaxy may be polluted with stellar detritus, tidal debris and globular cluster systems from the accretion of satellite galaxies with their own unique SFHs.

One prediction of hierarchical galaxy formation is that stellar halos should contain significant substructure in the form of tidal debris from past accretion events. Recently, good progress has been made in understanding the nature of halos built up by tidal stripping of accreted sub-halos through semi-analytic models (e.g., Bullock and Johnston (2005)) and numerical simulations (e.g., Helmi and White (1999)). Results predict significant amounts of stellar substructure distributed throughout the stellar halos of massive galaxies, with more recent events still having spatially coherent substructure (see figure 2).

Every satellite companion accreted is likely to have experienced different star formation and chemical enrichment histories; in the present day Local Group (LG) no two dwarfs have the same chemistry or star formation history (Grebel (2005)), so their partially digested remains, in the form of a coherent substructure, will contain stellar populations with distinct characteristics. In addition to polluting the stellar halo, satellite accretions can heat, thicken and even disrupt the stellar disk (Gauthier et al. (2006)). The closer we observe the stellar halos of galaxies within the local group, the more substructure we find (with the exception of M33). Ibata et al. (1994) discovered the extended tidal stream associated with the Sagittarius (Sgr) dwarf galaxy which is currently being cannibalised by the milky way. Figure 3 shows an image of a section of this stream from Belokurov et al. (2006). At least three other pieces of unrelated substructure are also visible.

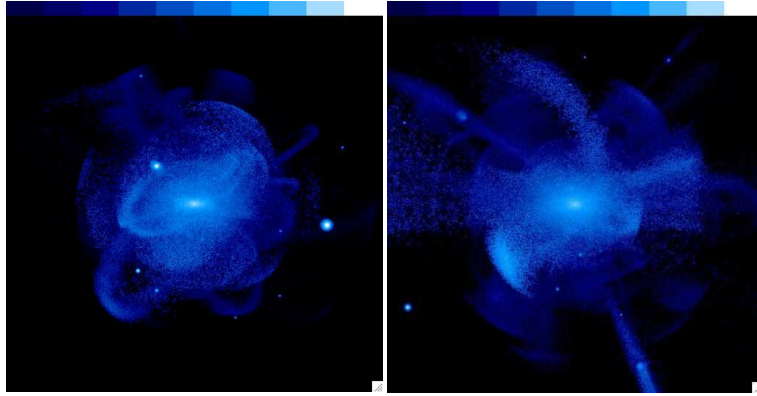


Figure 2: Examples of halo substructure formed from the accretion of ~ 100 dwarf satellites from simulations by Bullock and Johnston (2005). The blue shading represents stars from the accreted dwarf satellites only, and does not include halo stars belonging to the host galaxy. Surface brightness ranges from 23 mag/arcsec² (white) to 38 mag/arcsec² (blue). The boxes are 300kpc by 300kpc.

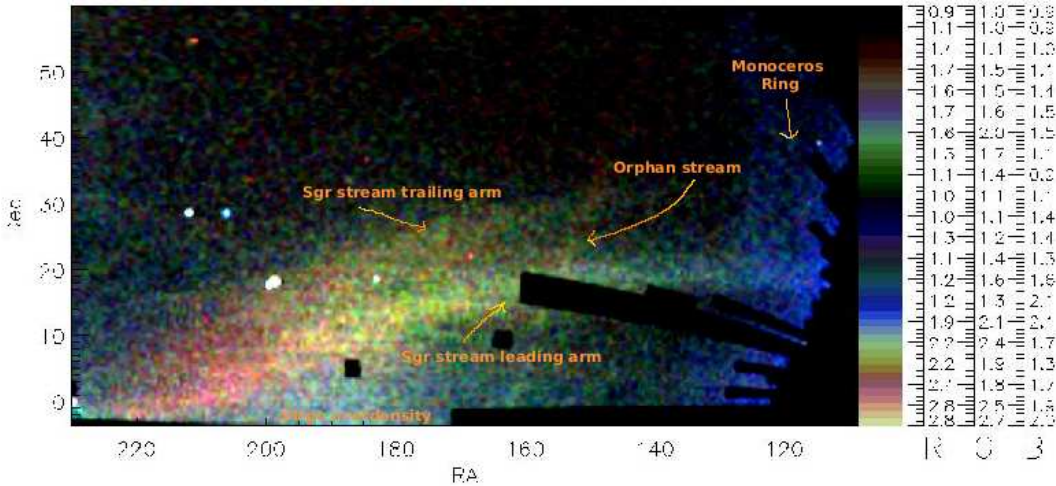


Figure 3: The spatial density of SDSS red giant branch stars created from 3 magnitude slices taken from Belokurov et al. (2006) and annotated. The colour coding refers to distance; blue stars are nearest to us, red stars are most distant and green stars are in between.

4 Stellar Evolution In the Colour Magnitude Diagram

The colour magnitude diagram (CMD) is perhaps the most powerful tool available for retrieving the fossil record of a population of stars. All that is required is deep photometry of a resolved stellar population in at least two filters and its distance (for stars further away than the Milky Way it is safe to assume that their line of sight distances within the target population are negligible compared to the distance of the field). The morphology of the observed CMD is interpreted in terms of the underlying physics of the parent population from which the star formation rate and chemical enrichment history can be determined.

The CMD is the observational counterpart to the Hertzsprung-Russell diagram (HRD; effective temperature vs luminosity) on which theoretical stellar evolutionary

tracks are plotted. The tracks are transformed into the observational plane using bolometric correction libraries. Although the most information is gleaned by measuring the best fit SFH of a CMD, rough constraints on the range of ages and metallicities present are possible by simply examining its shape or by comparing it to theoretical isochrones of known age and metallicity. An isochrone, meaning ‘same age’, is the curve of constant time that connects the evolutionary tracks of a SSP with identical metallicity and different initial masses. Stars occupy very specific loci on the CMD (figure 4) depending on their evolutionary phase.

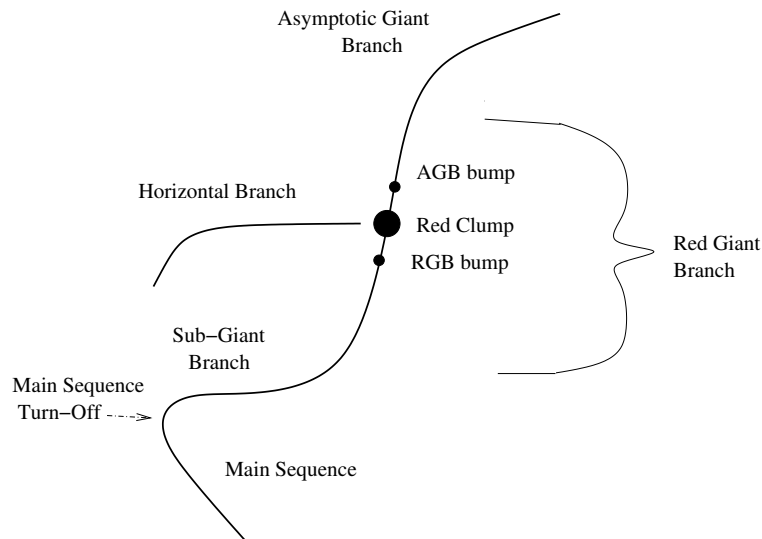


Figure 4: A rough sketch showing the loci of different evolutionary phases on the CMD.

When fitting the CMD we rely on our thorough (though not perfect) understanding of stellar evolution and how parameters such as metallicity, He content and mass loss affect them. A brief qualitative summary of the evolutionary phases highlighted in figure 4 follows:

- Along the **main sequence** (MS) stars burn H in their cores via the P-P chain. MS lifetime is strongly dependent on mass; the higher the mass, the shorter the time spent on the MS. Throughout this phase, the pressure steadily decreases (there are less free particles as H is converted into He) causing the star to slowly contract and heat up. At the same time, the opacity of He is less than the opacity of H so the luminosity increases monotonically.
- The **main sequence turn-off** (MSTO) is the bluest (hottest) point on a CMD. It marks the point where core H burning is terminated because the H within the core is exhausted. The position of the MS is an excellent age diagnostic if deep photometry down to the oldest MSTOs can be acquired.
- Along the **sub giant branch** (SGB) stars burn H in a shell around a HE core via the CNO cycle. The evolutionary rate for intermediate and high mass stars is so rapid during this phase that they are rarely observed. This absence of stars along the SGB is known as the ‘Hertzsprung gap’. Stars move from the blue

(hot) to the red (cooler) along the CMD as the core gradually contracts and the envelope expands, cools and increases in opacity. At some point, the cooling of the expanding outer layers causes the stellar envelope to become convective signalling the start of the RGB phase.

- Low mass stars on the **red giant branch** (RGB) burn H in a shell around a He core that is not dense enough to commence He burning. The core contracts and becomes degenerate. Mass loss is very efficient along the RGB. When the He added to it by shell H burning brings the core mass above a threshold value of $\sim 0.5M_{\odot}$. Core He burning starts violently and removes the degeneracy (the ‘He flash’) ending the stars lifetime on the RGB. RGB temperature depends strongly metallicity, although there is some age-metallicity degeneracy, making it a useful metallicity indicator. A CMD with a significant proportion of stars populating the RGB is representative of an old to intermediate aged population. Very high mass stars have non-degenerate cores and begin Ne burning without the aid of the He flash, failing to occupy the RGB.
- The **RGB bump** is a small overdensity of stars on the RGB due to stars crossing the same luminosity value three times as their H burning shells cross the pass the chemical discontinuity left behind by the expanding convective envelope causing a temporary drop in H burning efficiency.
- The evolution of core He (and H shell) burning stars proceeds differently for low and high mass stars. Low mass stars form the **horizontal branch** (HB), emerging from the RGB with almost identical masses and consequently luminosities. The effective temperature of HB stars is extremely sensitive to metallicity (amongst other things, not all of which are known) which is why the HB can cover a wide spread in colour for a relatively constant magnitude. In general, the more metal poor the population, the bluer the extent of the HB. Intermediate to high mass stars follow a separate track on the CMD known as the blue loop which usually has only a limited effect on the CMD.
- The **red clump** (RC) can be a very pronounced overdensity superimposed onto the RGB as a result of two overlapping phases. Primarily, it is the location of choice for the most metal rich, and therefore young to intermediate age, HB stars. It will also contain some stars from the faintest reach of the blue loop phase of core He burning intermediate mass stars.
- **Asymptotic giant branch** (AGB) stars burn He in a shell around a CO core, and H in a shell around that. For low and intermediate mass stars, the CO core mass is not sufficiently massive to ignite and becomes degenerate. It expands, producing a convective envelope akin to the RGB phase, and asymptotically approaches the RGB.
- The **AGB bump**) is caused by low mass stars beginning the AGB phase experiencing a small drop in luminosity when H burning in the outer shell ceases and the less efficient He shell ignites.

Figure 5, from Gallart et al. (2005), shows the locus on the CMD occupied by elementary populations with different age intervals but the same metallicity. This image

clearly highlights the weak dependence of the RGB on age and the Hertzsprung gap for young (i.e high mass) populations is evident. Very young stars form a plume on the blue side of the CMD and the oldest stars produce an extended horizontal branch. Increasing the metallicity would shift the tracks to the red. This can be used to make some distinctions about which features we expect to see on the CMD for populations of different ages:

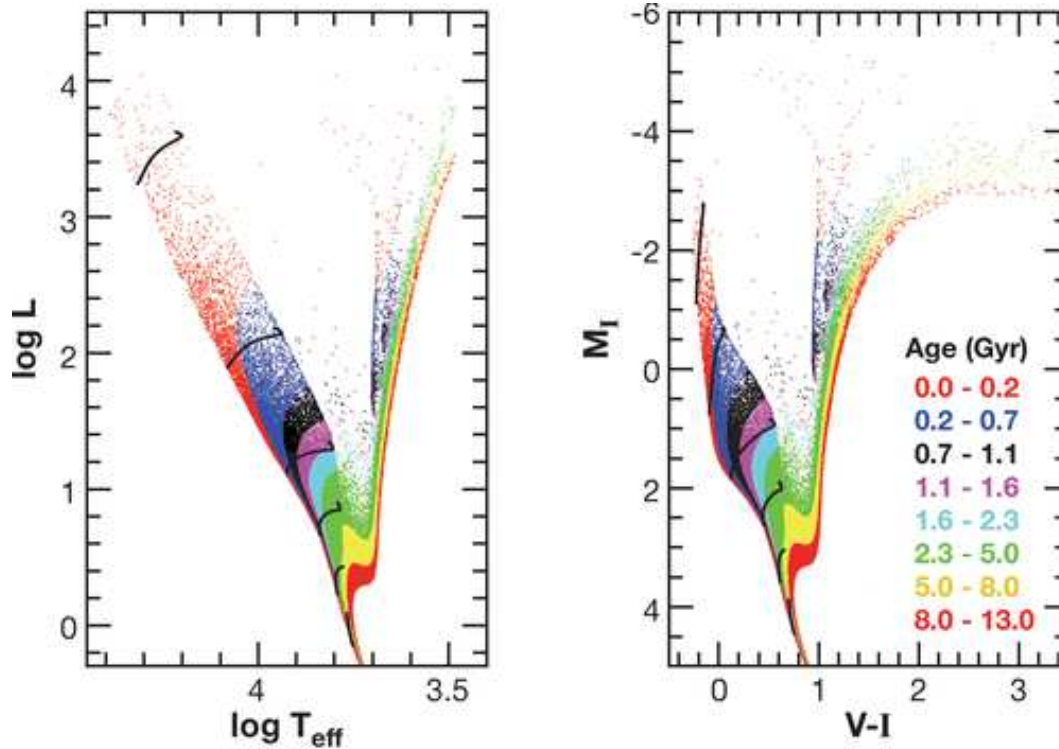


Figure 5: Synthetic CMD from Gallart et al. (2005) showing the area of the CMD different age intervals occupy in the theoretical (left) and observational (right) plane.

Old Populations: Age ≥ 10 Gyr. One would expect a well populated RGB but no AGB and possibly an extended blue HB.

Young Populations: Ages between 0 to 2Gyr. Such a population will display a strong blue plume of high mass MS stars, in young populations low mass stars are still unevolved and normally below detection thresholds. There will be no RGB but an AGB is possible.

Intermediate Populations: Ages between 2 and 10Gyr. Intermediate aged populations feature an RGB, AGB and usually a well populated RC too.

5 Interpreting Colour Magnitude Diagrams

So, now that we are fluent in reading CMDs, we can put the theory into practise.

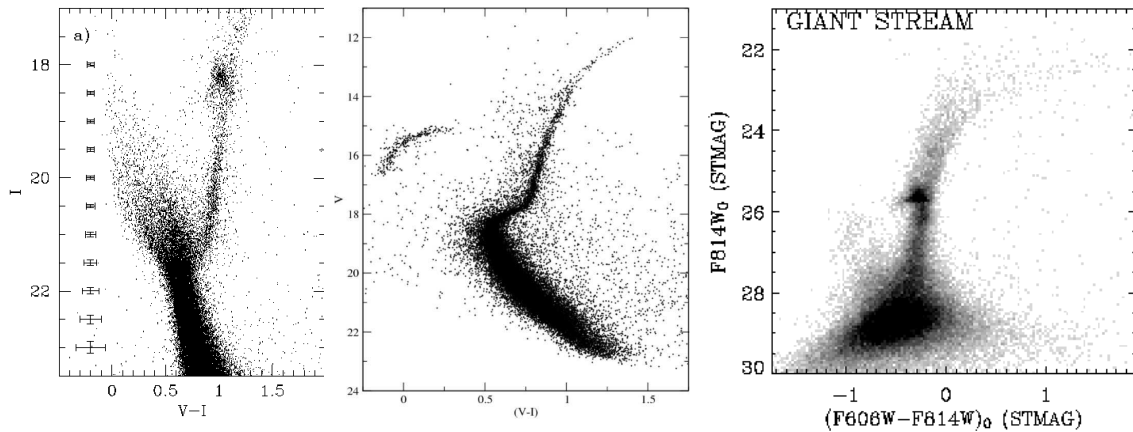


Figure 6: *Left* CMD of the LMC disk from Smecker-Hane et al. (2002). *Middle* CMD of globular cluster M92 from Paust et al. (2007). *Right* CMD of part of the giant stream in M31, from Ferguson et al. (2005)

The left panel of figure 6 is a CMD of a section of the LMC disk (Smecker-Hane et al. (2002)). Stars of all ages are present. There is a strong blue plume of very young main sequence stars, some intermediated aged stars (RC and RGB) and old stars (RGB).

The middle panel of figure 6 shows the CMD of globular cluster M92 (Paust et al. (2007)). It is obvious that this object is a globular cluster with essentially uniform age and metallicity because of the narrow spread in colour along the red giant branch and main sequence, and because of the sharp, coherent turn-off. For objects with extended star formation histories the multiple turn-offs blur out (e.g see left and right panels, figure 6). The long, blue extension of the horizontal branch tells us that this population is ancient and very metal poor.

The left panel of figure 6 is a CMD from a small section of the giant stream substructure in the stellar halo of Andromeda (M31) from Ferguson et al. (2005). There is no blue plume, so star formation within the last two Gyr is ruled out. The bulk of the stars appear to have intermediate ages (strong red clump overdensity). The well populated RGB indicates an intermediate to old population. The RGB is broad suggesting a range in metallicities, including some relatively metal-rich stars (red side of RGB). They may also be a small metal poor component (blue HB).

6 Finding the Best-Fit Star Formation History

Measuring the SFH from a CMD is akin to asking: What combination of star formation histories could have produced these observations? There are several subtle variations in the method employed for using photometric observations of a CSP to qualitatively determine the relative number of stars born as a function of age and metallicity (e.g., Harris and Zaritsky (2001), Aparicio and Gallart (2004), Dolphin (2002)). In brief, synthetic CMDs of simple stellar populations are fabricated using monte-carlo techniques and a linear combination of them is fit to the observed CMD to find the best fit star formation history. What follows is merely a cursory description of the general algorithm involved.

6.1 Ingredients

The main inputs needed are:

1. A stellar evolution library (theoretical isochrone set)
2. A bolometric correction library
3. Information about the binary fraction and ratio of primary to secondary mass
4. An initial mass function (IMF)
5. The distance modulus of the source
6. The interstellar extinction
7. Photometric errors
8. The completeness fraction as a function of magnitude

The adopted stellar evolutionary models are assumed to accurately represent represent the behaviour of stars with a particular mass, age and metallicity and to contain a theoretical counterpart to every population present in the observed population. The stellar evolutionary library supplies values of luminosity, effective temperature and surface gravity for a star with given mass, age and metallicity. A bolometric correction library is used to convert those parameters into magnitudes in the desired photometric system. Other information required as input are the distance modulus, interstellar extinction, photometric errors and completeness fraction as a function of magnitude (determined empirically) plus the initial mass function (IMF) and binary fraction. The latter two can either be estimated or fit along with the SFH.

6.2 Creating a realistic synthetic CMD

In the simplest scenario, the CEL and SFR are computed by linear interpolation between nodes of $Z(t)$ and $\psi(t)$ respectively. The total metallicity range is divided into m nodes of $Z(t)$ with a uniform distribution, hence constant CEL, between nodes. Likewise, the total age range is divided into n values of $\psi(t)$ with a constant SFR in each interval. Note that in this case the CEL approximates the moderate infall model.

A whole suite of ‘clean’ synthetic simple stellar population CMDs (j) are computed by first assigning random masses according to the prescribed IMF to a collection of stars using monte-carlo techniques. The total mass available to the system (M) is defined by the user. For every age value a synthetic CMD is made for all m metallicity values, giving a total of nm synthetic SSP CMDs. A star with a particular mass, age and metallicity has its effective temperature, luminosity and surface gravity calculated by interpolation within the stellar evolution library. In turn, interpolation of these values within a bolometric correction library yields magnitudes in the required photometric system. This is repeated on a star by star basis until the total mass, M , is reached for each of the nm populations. Some of the mass assigned may evolve out of the range covered by the isochrones - either because they are not massive enough or because they have evolved to non luminous end states (white dwarfs for example). The total mass limit should be very large to prevent small number statistics affecting short-lived evolutionary phases.

Each of the nm isochrones then represents the intrinsic photometry of a SSP with a specific age and metallicity. To enable a comparison with the observed CMD, the isochrones must be transformed into synthetic CMDs by accounting for the uncertainties in the observations. Firstly, the distance modulus, interstellar extinction, effects of unresolved binaries and blended stars is folded in. Secondly, it is essential to be in possession of detailed and accurate photometric errors and completeness fractions as a function of magnitude from artificial star tests, the results of which are used to consider the inclusion or removal of each star according to the completeness fraction at that magnitude. If retained, the stars photometric error is determined by those calculated for stars of that magnitude in the artificial star tests.

6.3 Determination of the Best Fit

Now a synthetic composite CMD is made from a linear combination of the simple stellar population CMDs providing the probability distribution from which the observed data are drawn. which can be compared to the data. The observed CMD and the synthetic CMD are both divided into identical grids with a total of N cells. Differential sized grid cells can be used to reduce the effect of poorly modelled evolutionary phases or to enhance the fitting of scarcely populated components. For example, if a small young population component is overlooked due to the presence of a densely populated RGB, enlarging the cells coinciding with the young population (those around the blue plume) ensures they will not be ignored during the fitting procedure. The number of stars located in cell i of the observed and synthetic CMDs are $N_{obs}(i)$ and $N_{syn}(i)$ respectively. Each SSP (j) contributes $N_j(i)$ stars to grid i of the composite synthetic CMD multiplied by its weight in the linear combination a_j so that

$$N_{syn}(i) = \sum_{j=1}^{nm} a_j N_j(i)$$

The amplitudes a_j denote the number of stars formed at the age and metallicity of the parent SSP. It is proportional to the star formation rate (in $M_{\odot}yr^{-1}$) experienced by that population. The fitting is achieved by using a merit function to compare the number of observed and synthetic stars in each cell:

$$\chi^2 = \sum_i^N \frac{(N_{obs}(i) - N_{syn}(i))^2}{N_{obs}(i)}$$

The above is true only in the case of Gaussian distributed observational errors. Since we are dealing with star counts, which can be very small in some cells, a Poisson distribution is more appropriate (Dolphin (2002)). If the probability of drawing $N_{obs}(i)$ from $N_{syn}(i)$ is

$$P(i) = \frac{N_{syn}(i)^{N_{obs}(i)}}{e^{N_{syn}(i)} N_{obs}(i)!}$$

then the ratio of the probability of drawing $N_{obs}(i)$ from $N_{syn}(i)$ to drawing $N_{obs}(i)$ from model $N_{obs}(i)$ is the Poisson likelihood ratio:

$$PLR(i) = \frac{N_{syn}(i)^{N_{obs}(i)} \times e^{N_{obs}(i)}}{N_{obs}(i)^{N_{obs}(i)} \times e^{N_{syn}(i)}}$$

The Poisson equivalent of χ^2 (Dolphin (2002)) is given by taking the log of the the cumulative likelihood ratio over all N cells

$$\ln PLR = \sum_i^N \left(N_{obs}(i) \ln \left(\frac{N_{syn}(i)}{N_{obs}(i)} \right) + N_{obs}(i) - N_{syn}(i) \right)$$

The actual merit function used varies between programs and depends on the quality of the data. The amplitudes associated with each SSP are varied until the best-fit star formation history is found. Thus the chemical enrichment law and star formation rate are known as functions of time.

7 Resources

- StarFISH package: For Inferring Star-formation Histories. Harris & Zaritsky, 2001 ApJS 136 25. <http://marvin.as.arizona.edu/jharris/SFH/>
- IAC-star synthetic CMD computation algorithm. Aparicio & Gallart (2004). <http://iac-star.iac.es/iac-star/>
- IAC-pop star formation history fitting program. Aparicio & Hidalgo (2007, submitted). http://www.iac.es/galeria/aa/j/iac-pop_eng.htm
- Padova isochrone database: <http://pleiadi.pd.astro.it/>

8 Bibliography

References

- Aparicio, A. and Gallart, C.: 2004, "Astronomical Journal" **128**, 1465
- Belokurov, V., Zucker, D. B., Evans, N. W., Gilmore, G., Vidrih, S., Bramich, D. M., Newberg, H. J., Wyse, R. F. G., Irwin, M. J., Fellhauer, M., Hewett, P. C., Walton, N. A., Wilkinson, M. I., Cole, N., Yanny, B., Rockosi, C. M., Beers, T. C., Bell, E. F., Brinkmann, J., Ivezić, Ž., and Lupton, R.: 2006, *Astrophysical Journal, Letters* **642**, L137
- Bullock, J. S. and Johnston, K. V.: 2005, *ApJ* **635**, 931
- Dolphin, A. E.: 2002, *Monthly Notices of the RAS* **332**, 91
- Ferguson, A. M. N., Johnson, R. A., Faria, D. C., Irwin, M. J., Ibata, R. A., Johnston, K. V., Lewis, G. F., and Tanvir, N. R.: 2005, *ApJ* **622**, L109
- Freeman, K. and Bland-Hawthorn, J.: 2002, *Annual Review of Astron and Astrophys* **40**, 487
- Gallart, C., Zoccali, M., and Aparicio, A.: 2005, *ARAA* **43**, 387
- Gauthier, J.-R., Dubinski, J., and Widrow, L. M.: 2006, "Astrophysical Journal" **653**, 1180

- Grebel, E. K.: 2005, in J. Mikolajewska and A. Olech (eds.), *AIP Conf. Proc. 752: Stellar Astrophysics with the World's Largest Telescopes*, pp 161–174
- Harris, J. and Zaritsky, D.: 2001, *ApJ* **136**, 25
- Helmi, A. and White, S. D. M.: 1999, *Monthly Notices of the RAS* **307**, 495
- Ibata, R. A., Gilmore, G., and Irwin, M. J.: 1994, *Nature* **370**, 194
- Paust, N. E. Q., Chaboyer, B., and Sarajedini, A.: 2007, *ArXiv Astrophysics e-prints*
- Smecker-Hane, T. A., Cole, A. A., Gallagher, III, J. S., and Stetson, P. B.: 2002, *"Astrophysical Journal"* **566**, 239